



## Persulfates to degrade a mixture of dyes (rhodamine B, methylene blue) in the presence of glucose and visible light

Piotr Zawadzki

Laboratory of Water and Sewage Technologies, Department of Water Protection, Central Mining Institute, Plac Gwarków 1, 40-166 Katowice, Poland, Tel.: 0048 32 259-28-01; email: pzawadzki@gig.eu

Received 2 June 2022; Accepted 21 December 2022

### ABSTRACT

A treatment process utilizing visible-light-activated (Vis) persulfates (PS) in the presence of an organic promoter (glucose) was developed for the simultaneous decolorization of a rhodamine B (RhB) and methylene blue (MB) mixture. Various doses of glucose, PS concentrations, pH values, initial dye concentrations and process time were tested to find out the most appropriate parameters for degrading the RhB/MB mixture in the PS/Vis/Glucose process. Under optimal conditions ( $C_{0[\text{RhB/MB}]} = 5$  ppm; pH = 4; glucose dosage = 230 mM; PS concentration = 30 mM; time = 120 min), the degradation of MB and RhB in the mixture was set to 87.8% and 54.7%. The degradation process followed the pseudo-first-order kinetic model with the correlation coefficient  $R^2 = 97\%–99\%$ . The PS/Vis/Glucose process is more economical than other existing studies and technologies. The energy efficiency at the optimal conditions were 1.2 and 2.1 kWh m<sup>-3</sup> for RhB and MB, respectively. The domination of MB degradation over RhB was confirmed and found to appear as a result of the different physico-chemical properties of the dyes and their state of charge, which enables the direct transfer of electrons from the dyes to the PS and leads to the decolorization of the dyes. This work provides an important source of information on the parameters influencing the simultaneous degradation of mixtures of dyes (rhodamine B, methylene blue). The experimental results showed that the PS/Vis/Glucose process may have a positive role in treating color solution mixtures with various dye concentrations (1–20 ppm).

*Keywords:* Rhodamine B; Methylene Blue; Advanced oxidation process; Sodium persulfate; Glucose; Visible light

### 1. Introduction

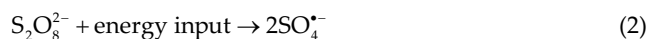
Industrial wastewater contains a broad range of various chemical compounds that can be by-products of conducted technical processes (e.g. dyes, phenols, pesticides, heavy metals). The textile, chemical, food and tanning industries generate the greatest quantities of industrial wastewater containing synthetic dyes such as methylene blue (MB) and rhodamine B (RhB) [1]. MB and RhB are heterocyclic dyes that find broad application in the industry; however, they contribute to significant environmental problems due to their high toxicity and accumulation in the environment.

Methylene blue belongs to the azo dye group. Azo dyes are histamine-releasing agents, therefore exposure to them may result, for example, in urticaria or intensified symptoms of asthma as well as uterine contractions in pregnant women, leading to miscarriage [2]. Rhodamine B is used in the chemical, textile, paper and paint industries. The negative influence of RhB on humans and animals manifests itself as skin, eye and respiratory system irritation. RhB also exhibits potential mutagenic and carcinogenic effects [3].

Due to their hazardous influence on humans and high resistance to biodegradation, it is necessary to develop a technology for eliminating dyes from water and wastewater.

Several dyes treatment methods have been developed, including physical (membrane processes, adsorption) [4,5], chemical (ozonation, chlorination) [6,7] and biological processes (aerobic, anaerobic, microbial biosorbents) [8,9] as well as combined methods (e.g., physical and chemical) [10]. The currently applied methods do not come without a drawback. For example, physical methods do not eliminate the hazard, but rather usually transfer it into a different phase (e.g., concentrate in membrane processes). On the other hand, biological methods are sensitive to high pollutant concentrations and wastewater composition variations.

Advanced oxidation processes (AOPs) are an interesting alternative to conventional treatment methods. A common feature of AOPs is the chemical reaction between oxidative radicals and organic pollutants. In recent years, significant attention has been devoted to sulfate radicals ( $\text{SO}_4^{\bullet-}$ ) [11]. The radical precursor of  $\text{SO}_4^{\bullet-}$  (persulfate (PS)) requires activation to generate sulfate radicals. The chemical structure of PS is  $[\text{O}_3\text{S}-\text{O}-\text{O}-\text{SO}_3]^{2-}$ . The essence of the persulfate activation mechanism is the excitation of PS, the break of the  $-\text{O}-\text{O}-$  bond and the production of  $\text{SO}_4^{\bullet-}$  radical with a high oxidative potential ( $E^0 = 2.6-3.1\text{V}$ ) [12,13]. The persulfate requires activation. PS activation is often carried out by expensive, energy-consuming and complex activation methods, for example, by UV radiation, base activation ( $\text{pH} > 11$ ), thermal methods, and low oxidation transition metal ions (e.g.,  $\text{Fe}^0$ ,  $\text{Fe}^{2+}$ ,  $\text{Ag}^+$ ,  $\text{Co}^{2+}$ ,  $\text{Cu}^{2+}$ ). Activation via transition metal ions generates a single sulfate radical [Eq. (1)]. Activation by UV or heat results in the production of two sulfate radicals [Eq. (2)].



The disadvantage of activation by UV radiation is the power of the used lamps, which often exceeds 100 W, and sometimes even 400 W [14]. Base activation requires large amounts of chemical reagents due to the high pH, then decrease of the pH to a value that is required under the applicable regulations. On the other hand, disadvantages of activation via transition metal ions include the cost of the reagents as well as iron sludge generation due to the application of ferrous ions.

A simple and economic method of activation is the combination of PS activation processes in the presence of glucose and visible light (Vis). First of all, visible light is a free source of energy. The cost of electricity in the industrial and municipal facilities (wastewater treatment plant) is one of the primary factors determining the cost-effectiveness of investments and the treatment costs of 1 m<sup>3</sup> of wastewater. Then, glucose is an organic activator of PS, and its price might be even twice lower compared, for example, to  $\text{FeSO}_4 \cdot 7\text{H}_2\text{O}$ , which finds common application in PS activation. Therefore, organic promoters such as glucose decrease the operational costs, shorten the reaction time and increase the degradation efficiency [15].

Most research that assesses novel technologies evaluates the process efficiency based on a single dye [16–21]. There are few studies dedicated to the simultaneous degradation of mixtures of various compounds [22–24]. This is significant

because dyes are typically found in colored mixtures. The presence of various dyes can both intensify or weaken the pollutant degradation process. Therefore, this study presents an evaluation of the PS/Vis/Glucose process efficiency based on the simultaneous degradation of two dyes: rhodamine B and methylene blue.

The novelty of the present work lies in its simplicity by which a mixture of dyes can be degraded using non-toxic, pro-environmental reagents (glucose) and low-cost solar energy (visible light) with higher process efficiency. The dye mixture decolorization experiments with the use of PS in this study were conducted using various environmental parameters, such as different doses of glucose, PS concentrations, pH values, initial dye concentrations and process time, to find out the most appropriate parameters for degrading RhB/MB in the presence of visible light. The paper would acquaint the readers to the important source of information on the parameters influencing the simultaneous degradation of mixtures of dyes (rhodamine B, methylene blue). The novelty in the paper includes an attempt to explain the mechanism of interaction between two dyes: rhodamine B and methylene blue in mixture, proving to be a knowledge pool and helping the researchers working in the similar field to design appropriate treatment plans for real textile wastewater.

## 2. Materials and methods

### 2.1. Dyes

Rhodamine B with a purity  $\geq 95.0\%$  and methylene blue with a purity  $\geq 97.0\%$  were provided by Sigma-Aldrich (Poznań, Poland). The model solutions were prepared based on deionized water as well as RhB and MB standard additions. The structures of the used dyes are presented in Fig. 1.

### 2.2. Analyses

The decolorization effect was assessed via absorbance measurement by Jasco V-750 spectrophotometer (Kraków, Poland) over a range of 400 to 800 nm. Fig. 2 presents the absorption spectra obtained for a RhB/MB mixture with an initial concentration of 1 ppm. The RhB absorption spectrum exhibits a maximum peak at  $\lambda_{\text{max}} = 554$  nm. The MB absorption spectrum exhibits a maximum peak at  $\lambda_{\text{max}} = 665$  nm.

The degree of dye mixture decolorization was determined based on characteristic absorption peaks at 554 nm (RhB) and 665 nm (MB). In order to determine the decolorization efficiency, the absorption was measured before and after AOPs, as shown in Eq. (3), where:  $C_0$  – initial concentration,  $C_t$  – concentration at time  $t$ .

$$\text{Decolorization efficiency (\%)} = \frac{C_0 - C_t}{C_0} \quad (3)$$

### 2.3. Experimental procedure

#### 2.3.1. Source of visible light

A 10 W tungsten lamp emitting visible light (400–2,200 nm), model QTH10/M (Thorlabs Inc., USA), was

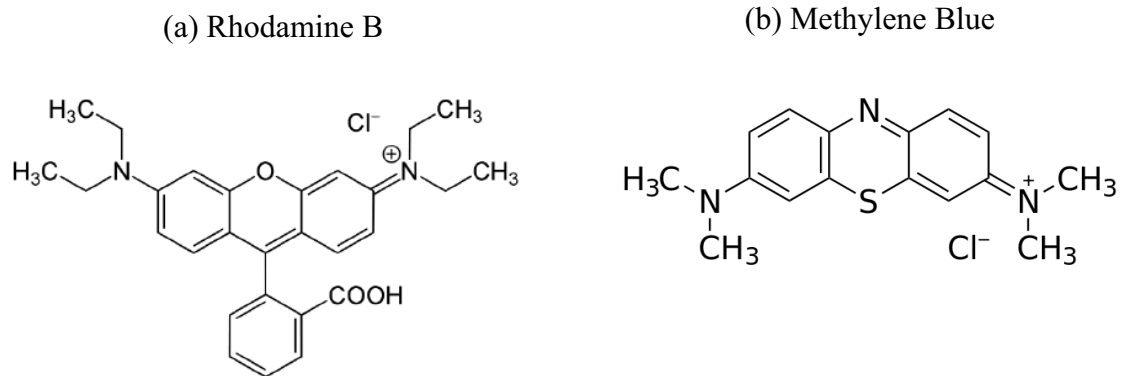


Fig. 1. Structure of Rhodamine B (a) and structure of Methylene Blue (b).

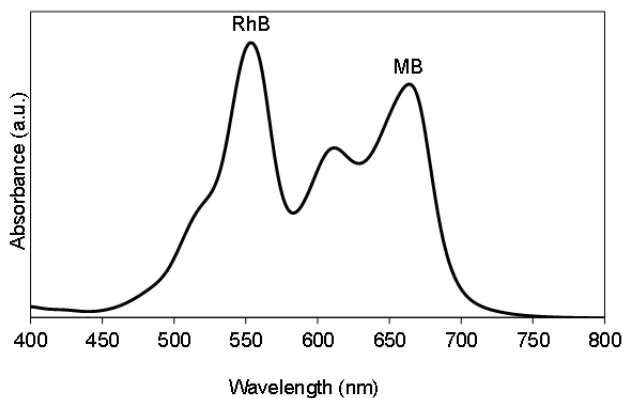


Fig. 2. Absorption spectrum of rhodamine B and methylene blue mixtures.

used for the dye mixture degradation tests. A FGS900M filter (Thorlabs Inc., USA) was applied to cut off the spectrum bands above 710 nm. All the experiments were conducted in vessels with a volume of 0.2 dm<sup>3</sup>, without the possibility of exposure to additional light sources.

### 2.3.2. Effect of glucose and PS

The influence of the initial glucose dosage and the initial PS concentration were examined. The following parameters were constant: RhB/MB concentration ( $C_{0[\text{RhB/MB}]}$ ) = 1 ppm, time = 70 min, pH = 6, room temperature. The influence of the initial glucose dosage was examined at a PS concentration = 20 mM and various doses of glucose: 140, 170, 200, 230, 260 and 290 mM. The influence of the initial PS concentration was examined at a glucose concentration = 230 mM and various PS concentrations: 15, 20, 25, 30, 35 and 40 mM.

### 2.3.3. Effect of pH

The influence of the initial pH of the aqueous solution was studied. The following parameters were constant:  $C_{0[\text{RhB/MB}]}$  = 1 ppm, time = 70 min, room temperature, dose of glucose = 230 mM, PS concentration = 30 mM. The solutions were corrected to pH values of 4, 5, 6, 7, 8, 9 and 10. The pH was corrected with 0.1 mol dm<sup>−3</sup> HCl or 0.1 mol dm<sup>−3</sup> NaOH

provided by Sigma-Aldrich. The pH of the model solution was measured using an Elmetron CPC-511 pH meter (Zabrze, Poland).

### 2.3.4. Effect of dyes concentration

The influence of the initial RhB/MB concentration was also examined. The following parameters were constant: time = 70 min, room temperature, dose of glucose = 230 mM, PS concentration = 30 mM, pH = 6. The following dye concentrations were tested: 1, 5, 10, 15 and 20 ppm.

All the experiments were conducted independently and repeated in triplicate, similarly to other studies involving persulfates [25]. The data presented in the next sections include average values.

## 2.4. Reaction kinetics

A pseudo-first-order kinetic model [Eq. (4)] was used to describe the kinetics, similarly to the study [26].

$$-\ln\left(\frac{C}{C_0}\right) = kt \quad (4)$$

where  $C_0$  – RhB/MB concentration before the treatment process (ppm);  $C$  – RhB/MB concentration after the treatment process (ppm);  $k$  – reaction rate constant (−);  $t$  – reaction time (min).

## 2.5. Energy consumption

Electricity consumption is one of the essential criteria in the water and wastewater treatment process. To compare the cost of the current study with other existing studies and technologies, electricity consumption was estimated based on the electric energy per order indicator ( $E_{\text{EO}}$ ). For the electrochemical degradation processes, the energy efficiency ( $E_{\text{EO}}$ ), expressed as kWh m<sup>−3</sup> of treated solution, was calculated based on the anode surface area ( $S$ , cm<sup>2</sup>), the applied current density ( $i$ , mA cm<sup>−2</sup>), the applied average voltage ( $U$ , V), and the reaction volume ( $V$ , dm<sup>3</sup>), as shown in Eq. (5) [27].

$$E_{\text{EO}} \left( \text{kWh m}^{-3} \right) = \frac{S \cdot i \cdot U}{(t/V) \cdot 1000} \quad (5)$$

For the photochemical degradation, the  $E_{EO}$  was calculated with the following equation [Eq. (6)] [28,29]:

$$E_{EO} (\text{kWh m}^{-3}) = \frac{P \cdot t \cdot 1,000}{\log[C_0 / C_t] \cdot V \cdot 60} \quad (6)$$

where  $P$  – the electrical power consumed by lamp (kW);  $t$  – the process time (h);  $C_0$  – the initial concentration of the dye (ppm);  $C_t$  – the concentration of the dye after  $t$  (ppm);  $V$  – the reaction volume ( $\text{dm}^{-3}$ ).

### 3. Results and discussion

#### 3.1. Effect of glucose dose on degradation of dyes mixture

As shown in Fig. 3, increasing the glucose dosage results in higher dye mixture decolorization efficiency. For further experiments, a concentration of 230 mM was selected as the optimal dose of glucose. Under optimal conditions, the decolorization degree was the highest for RhB (43.8%). Exceeding a dose of 200 mM did not result in a significant effect of MB removal. Therefore, due to the weaker decolorization effect in the case of RhB, the 230 mM dose was considered to be the most effective.

To increase the persulfate activity in visible light, sugars (e.g., glucose, sucrose) are used in the decolorization technology [30,31]. For example, glucose is an optically active substance and a donor of electrons that may activate PS. The mechanism of activation by glucose is similar to activation by phenoxides. The electron from glucose is transferred to the persulfate and activates it. On the other hand, glucose could be oxidized into products that may activate the persulfate. This is connected to organic PS activation through an external carbon source [32]. Lower doses of glucose showed unsatisfactory decolorization effect. Higher doses inhibited the decolorization effect since the glucose is also used as a free radical scavenger ( $k_{OH\cdot} = 1.5 \times 10^9$ ) [33].

#### 3.2. Effect of PS dose on degradation of dyes mixture

Similarly to glucose, the PS concentration has a significant influence on the RhB/MB degradation. Therefore the influence of initial PS concentrations on the decolorization

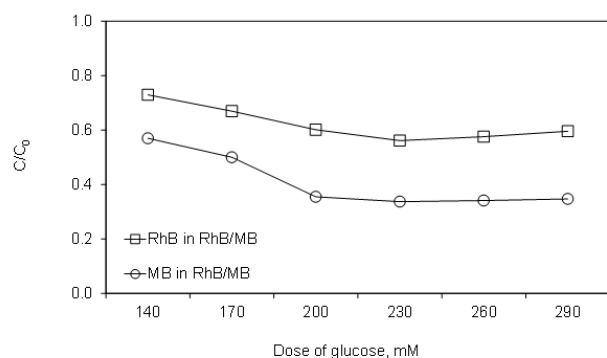


Fig. 3. The dyes mixtures decolorization effect at different glucose dose. Experimental conditions:  $C_{0[\text{RhB/MB}]} = 1$  ppm;  $\text{pH} = 6$ ; reaction time = 70 min; PS concentration = 20 mM.

efficiency was studied as well. Fig. 4 demonstrates that after 70 min, the initial dye mixture concentration was reduced by a range of about 12%–38% in (RhB) and by about 38% to 67% (MB). Under the operating conditions, the greatest decolorization effect for both dyes was achieved at a PS concentration of 30 mM. Similarly to the study [26], the PS concentration above 30 mM resulted in lower methylene blue decolorization efficiency. This phenomenon also occurs in the case of photocatalytic processes. Mahanthappa et al. [34] studied the influence of a different doses of the CuS-CdS catalyst ( $40\text{--}240 \text{ mg dm}^{-3}$ ). The level of methylene blue removal ranged from 40% to nearly 100%. The highest removal degree was observed at a dose of  $200 \text{ mg L}^{-1}$  (almost 100%). Higher doses of the catalyst most likely result in nanoparticle aggregation and faster sedimentation. In this study, higher PS concentration resulted in a higher density of the generated oxidative components. After exceeding the optimal PS concentration (30 mM), the decolorization efficiency decreased, most likely due to the reaction between the sulfate anion and hydroxyl radicals [35] [Eqs. (7) and (8)].



#### 3.3. Effect of different RhB and MB concentrations

This study shows that increasing concentrations of the dye molecules disrupt the process in which free radicals are involved. Fig. 5 confirms that the effect of the RhB/MB decolorization depends on the dye concentration. Increasing the concentration from 1 to 20 ppm resulted in a nearly twofold decrease in the decolorization efficiency. Bagherzadeh et al. [36] studied the influence of the initial MB concentration on the degradation efficiency. With the increasing MB concentration from 10 to 20  $\text{mg L}^{-1}$ , a decrease in the degradation rate from 92% to 73% was observed. As the concentration increases, the oxidative radical consumption becomes greater, whereas the likelihood of a collision between the oxidative radicals and the dye molecules decreases. Han et al. [37] also investigated the influence of the MB concentration on the final decolorization effect and confirmed that

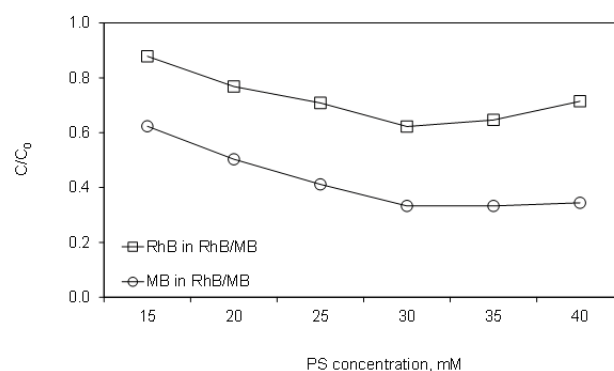


Fig. 4. The dyes mixtures decolorization effect at different PS concentration. Experimental conditions:  $C_{0[\text{RhB/MB}]} = 1$  ppm;  $\text{pH} = 6$ ; reaction time = 70 min; glucose dose = 230 mM.

higher dye concentrations inhibit radical reactions with the dye molecules. Chen et al. [38] also proved this relationship for RhB. Furthermore, a high molecule concentration can result in effects of competition between the dye molecules, reaction products and generated radicals.

### 3.4. Effect of pH on degradation of dyes mixture

The pH significantly influences the direction of radical generation, and consequently on the degradation rate. Fig. 6 shows the decolorization rate at various pH. After 70 min, the maximum decolorization efficiency of 64% and 83% for RhB and MB, respectively was achieved at pH = 4. At higher pH (6), the decolorization efficiency decreased to about 38% (RhB) and 62% (MB). At pH = 10, the decolorization efficiency decreased to about 21% (RhB) and 41% (MB). This is a result of the participation of various oxidative radical forms depending on pH. Sulfate radicals dominate at pH < 7, whereas an increase in pH results in the generation of hydroxyl radicals ( $\text{OH}^\cdot$  concentration >  $10^{-7}$ ). Thus, the removal efficiency decreases due to the scavenging of the  $\text{SO}_4^{\cdot-}$  radicals by  $\text{OH}^\cdot$  [39]. Similar conclusions were presented by Oliveros et al. [40].

The degradation of methylene blue was more effective than rhodamine B. MB is a cationic dye at a pH range

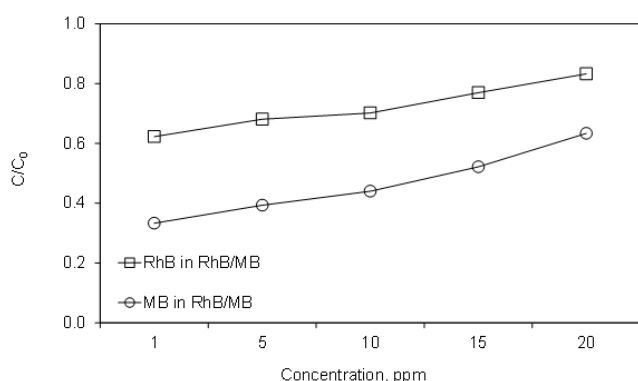


Fig. 5. Influence of different RhB and MB concentration on the decolorization effect. Experimental conditions: pH = 6; reaction time = 70 min; glucose dose = 230 ppm; PS concentration = 30 mM.

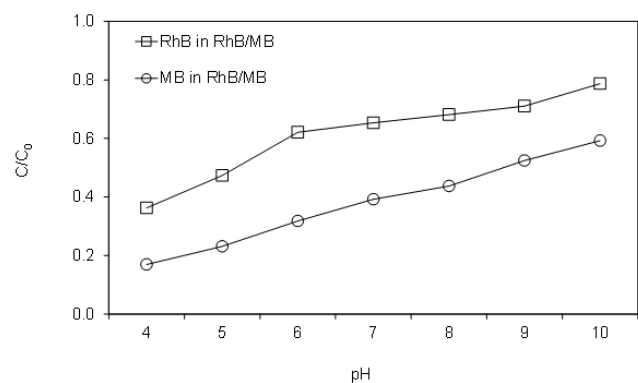


Fig. 6. RhB and MB decolorization effect at different pH. Experimental conditions:  $C_{0[\text{RhB/MB}]}$  = 1 ppm; reaction time = 70 min; glucose dose = 230 ppm; PS concentration = 30 mM.

of 1.7–8.0 [41,42], whereas RhB has two molecular forms (cationic and zwitterionic) [43]. This means that a dissociated RhB molecule transfers charges from positive to neutral together with the increase in pH. Therefore a likely reason for this phenomenon may be found in the dyes' state of charge at various pH. It may result in the direct transfer of electrons from the dyes to the PS, which in turn is responsible for the dye decolorization. Sodium persulfate (a source of  $\text{SO}_4^{\cdot-}$  radicals) dissociates to generate  $\text{S}_2\text{O}_8^{2-}$  ion with two negative charges. MB may dissociate cations that bond with electronegative substances in an aquatic solution. Therefore the decolorization rate was higher for MB and lower for RhB [44,45]. For this reason, it is recommended to apply a pH value of 4 for the decolorization of the RhB/MB mixture in the PS/Vis/glucose process.

### 3.5. Degradation kinetics and efficiency

The effectiveness of the PS/Vis/Glucose technology was demonstrated by performing a degradation test for single dye (RhB and MB separately) and a dye mixture (RhB/MB). The degradation experiments were carried out at a concentration of 5 ppm, since the PS/Vis/Glucose technology was designed for this concentration range. The decolorization tests were performed under optimal conditions: pH = 4; glucose dosage = 230 mM; PS concentration = 30 mM. The process was carried out for 120 min. Fig. 7 shows the influence of time on the degree of RhB, MB and RhB/MB mixture decolorization. The decolorization degree increased together with the process duration. For example, after 20 min of the reaction, the efficiency was set to 13.1%, 44.9%, 28.3% and 10.2%, respectively for RhB (alone), MB (alone), and MB and RhB in a mixture. A satisfactory decolorization degree was obtained after 120 min. The efficiency was set to 62.8%, 95.6%, 87.8% and 54.7%, respectively for RhB (alone), MB (alone), and MB and RhB in a mixture.

As the degradation proceeds, sulfate radicals generate (Eq. (9)). Persulfate activation is the result of a synergistic reaction between the visible light and the intensified effect of electron transfer from the glucose to the persulfate. Glucose tends to rotate the plane-polarized light and is active in visible light. Glucose is also an electron donor in the PS/Vis system. It is very strongly soluble in water and facilitates

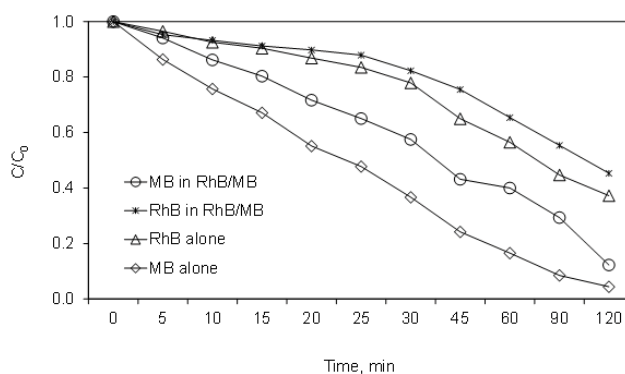
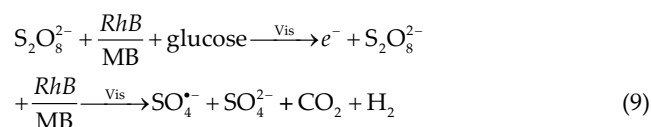


Fig. 7. Decolorization effect ( $C/C_0$ ) of the RhB, MB and RhB/MB mixture. Experimental conditions:  $C_{0[\text{RhB/MB}]}$  = 5 ppm; pH = 4; glucose dose = 230 mM; PS concentration = 30 mM.

persulfate activation, as its functional groups (e.g., the carbonyl group) partially receive the negative charge.



Furthermore, under operating conditions, sulfate radicals dominate at pH = 4 [39]. Sulfate ions and free hydroxyl radicals are generated as a result of the reaction of free sulfate radicals with hydroxyl ions [Eq. (10)].



Significant differences in decolorization efficiency were observed between RhB, MB and the RhB/MB mixture. It was found that the degradation efficiency was greater both in the case of the single MB dye and the RhB/MB solution compared to the RhB degradation. Furthermore, the RhB/MB degradation rate was higher than in the case of RhB, which was also confirmed by Sharma and Khare [46].

One of the possible reasons for this may be the physico-chemical characteristics of the dyes. At 25°C, RhB is less soluble in water than MB (MB = 43.6 g dm<sup>-3</sup> vs RhB = 10 g dm<sup>-3</sup>). On the other hand, Rani et al. [47] concluded that the effective degradation of RhB requires a more basic solution compared to MB when applying catalysts such as ZnO<sub>2</sub>.

Another reason may also arise from the lower Vis radiation absorption of the RhB dye. The Vis radiation intensity is sufficient to achieve a more significant PS activation and oxidation of MB compared to RhB [48].

The degradation of the RhB and MB mixture in the PS/Vis/Glucose process results from chemical reactions. It is briefly presented in Fig. 8. The absorbance intensity decreased during the time duration of the experiment with PS/Vis/Glucose. The primary rhodamine B degradation mechanism include the N-deethylation process, chromophore cleavage and ring opening, which result in the generation of oxidation products with smaller molecule sizes [49–51]. In turn, Mostafa Mahdavianpour et al. [52] suggested that the degradation of azo bonds is a possible mechanism of MB decolorization. On the other hand, Yang et al. [41] proposed a similar mechanism consisting of the initial formation of a complex between MB ions and a S<sub>2</sub>O<sub>8</sub><sup>2-</sup> ion as a result of electrostatic attraction. Afterward, this may lead to a direct transfer of electrons from MB to the PS, which is most likely the phenomenon responsible for the decolorization of methylene blue.

The decolorization rate constant is presented in Fig. 9. The correlation coefficient R<sup>2</sup> showed a very good fit of experimental data (R<sup>2</sup> = 97%–99%). Considering the low concentration of the organic molecule, the dye decolorization followed the pseudo-first-order kinetic model, as also shown in [53–55]. The mathematically calculated half-life (t/2) was set to 79.7, 26.1, 103.5 and 42.5 min, respectively for RhB (alone), MB (alone), RhB in RhB/MB and MB in RhB/MB.

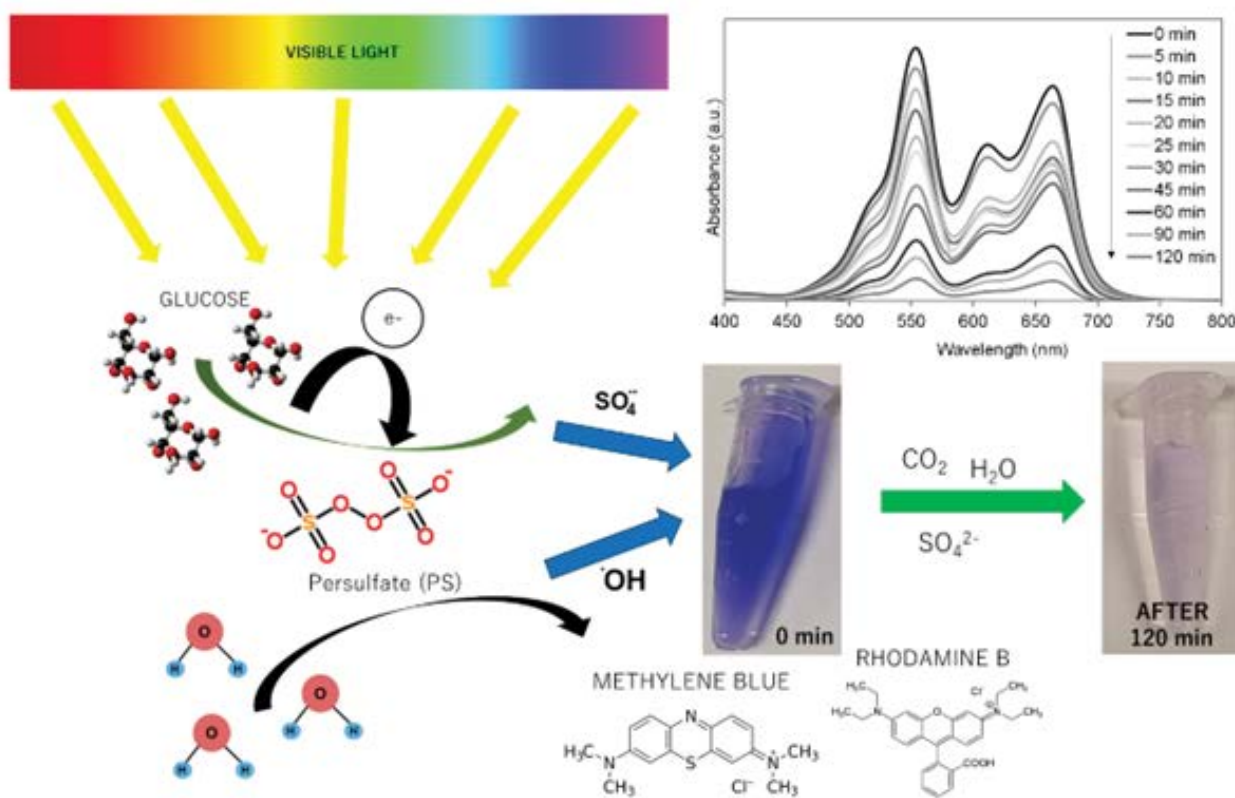


Fig. 8. Proposed summary of visible-light activation of persulfate for RhB/MB decolorization.

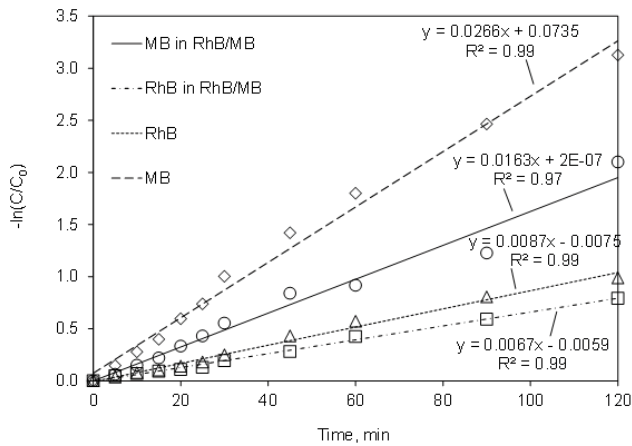


Fig. 9. Kinetic constants of the RhB, MB and RhB/MB decolorization. Conditions:  $C_{0[\text{RhB/MB}]} = 5$  ppm; pH = 4; glucose dose = 230 mM; PS concentration = 30 mM.

#### 4. Comparison with other AOPs systems

The proposed decolorization method (PS/Vis/Glucose) is a promising treatment technology for dye mixtures with concentrations of up to about 5 ppm. As presented in Table 1, the proposed technology is an interesting alternative to other methods that are commonly used to remove dyes. After 120 min of decolorization by PS/Vis/Glucose, the degradation of MB and RhB in a dye mixture was set to 87.8% and 54.7%. This time was shorter than [56], where 97.7% of RhB was removed after 180 min of reaction time. In the PS/Vis/Glucose process it is also possible to achieve a higher decolorization effect over a shorter process, time compared to the study [57], where 51% of RhB was removed after 180 min. A very important advantage of the PS/Vis/Glucose process is low energy consumption since a low-power radiation source (10 W) was used. Rokesh et al. [58] achieved 60% of RhB decolorization despite using a lamp with a power of 300W. The proposed technology is also waste-free, compared to [59], which

Table 1  
Efficiency of Rhodamine B and Methylene Blue degradation in different AOPs

Process	Target pollutant	Conditions	Removal efficiency [%]	$E_{\text{EO}}$ [kWh m <sup>-3</sup> ]	References
PS/Vis/Glucose	Rhodamine B	$C_{0[\text{RhB}]} = 1$ ppm Time = 70 min PS dose = 30 mM Glucose dose = 230 ppm Lamp power = 10W Reaction volume = 0.2 dm <sup>-3</sup>	64	2.1	This study
PS/Vis/Glucose	Methylene Blue	$C_{0[\text{MB}]} = 1$ ppm Time = 70 min PS dose = 30 mM Glucose dose = 230 ppm Lamp power = 10W Reaction volume = 0.2 dm <sup>-3</sup>	83	1.2	This study
PS/Vis/Glucose	Methylene Blue	$C_{0[\text{MB}]} = 2$ ppm Time = 90 min PS dose = 0.065 mM Glucose dose = 100 ppm Lamp power = 10W Reaction volume = 0.1 dm <sup>-3</sup>	65	4.8	[15]
PS/Vis/Ultrasound	Rhodamine B	$C_{0[\text{RhB}]} = 10$ ppm Time = 60 min PS dose = 20 mM Glucose dose = 200 ppm Lamp power = 10W pH = 6.0 Reaction volume = 0.5 dm <sup>-3</sup> T = 295 K	85	0.4	[51]
Ti/SnO <sub>2</sub> -Sb electrode	Rhodamine B	$C_{0[\text{RhB}]} = 50$ ppm pH = 3.0 Time = 20 min Current density = 20 mA/cm <sup>2</sup> Applied average voltage = 8.9 V Na <sub>2</sub> SO <sub>4</sub> = 10 mmol/L Reaction volume = 0.03 dm <sup>-3</sup>	97.8	80.1	[27]

Table 1 (Continued)

Table 1

Process	Target pollutant	Conditions	Removal efficiency [%]	E <sub>EO</sub> [kWh m <sup>-3</sup> ]	References
Peroxide assisted photocatalytic degradation in the presence of ZnO	Rhodamine B	C <sub>0[RhB]</sub> = 5 ppm Time = 90 min ZnO = 500 ppm Reaction volume = 0.05 dm <sup>-3</sup> Lamp power = 300W	60	326.7	[58]
Photo-Fenton processes	Methylene Blue/ Brilliant Green/ Eosin Yellow	C <sub>0[dyes]</sub> = 1 ppm Time = 60 min pH = 3 Fe <sup>2+</sup> = 4.5 ppm H <sub>2</sub> O <sub>2</sub> = 13.06 mM Lamp power = 160 W Reaction volume = 0.25 dm <sup>-3</sup> Temperature = 25°C	80	15,3	[53]
Electro-Fenton	Rhodamine B	C <sub>0[RhB]</sub> = 10 ppm pH = 2 Time = 180 min Electrode dose = 15 ppm Voltage = 8 V	97.7	n.d.	[56]
UV-LED/TiO <sub>2</sub>	Rhodamine B	C <sub>0[RhB]</sub> = 49 ppm Time = 180 min pH = 3.05 TiO <sub>2</sub> = 1.6 g dm <sup>-3</sup> Lamp = 5 × LED Luminous intensity = 350 mcd Radiant flux = 10–12 mW at 20 mA	51	n.d.	[57]
Fe(0)-based Fenton process with H <sub>2</sub> O <sub>2</sub>	Rhodamine B	C <sub>0[RhB]</sub> = 49 mg/L Time = 30 min pH = 4 Fe(0) = 1 g/L H <sub>2</sub> O <sub>2</sub> = 2 mM	100	n.d.	[59]
Electrochemical degradation in the presence of sulphate ions	Methylene Blue	C <sub>0[MB]</sub> = 21 ppm Time = 180 min Room temperature Sulphate ions concentration = 0.1 ppm	73	n.d.	[60]

n.d. – no data

utilized the Fenton reagent. The main disadvantages of the Fenton reagent are the relatively high cost of H<sub>2</sub>O<sub>2</sub> and the formation of iron sludge. As shown in Table 1, it can be seen, the PS/Vis/Glucose process is more economical than other existing studies and technologies. The energy efficiency at the optimal conditions were 1.2 and 2.1 kWh m<sup>-3</sup> for RhB and MB, respectively. However, it should be noted that the calculated values refer only to the conversion of UV radiation. For detailed calculations, other parameters such as electricity consumption of ozone generator, chemical consumption, mixing, and other factors should be considered.

## 5. Conclusions

The study presented an evaluation of the PS/Vis/Glucose process efficiency based on the degradation of two dyes:

rhodamine B and methylene blue. The simultaneous degradation of dyes dissolved in an aquatic solution was investigated. The dye degradation process was modelled by testing the influence of various process parameters (different doses of glucose, PS concentrations, pH, initial dye concentrations, process durations) to find out the most optimal conditions for RhB/MB degradation in the presence of visible light and an organic promoter (glucose). Under optimal conditions (C<sub>0[RhB/MB]</sub> = 5 ppm; pH = 4; glucose dosage = 230 mM; PS concentration = 30 mM; time = 120 min), the degradation of MB and RhB in the mixture was 87.8% and 54.7%. The dye degradation followed the pseudo-first-order kinetic model with the correlation coefficient R<sup>2</sup> = 97%–99%. PS/Vis/Glucose process was also the most effective process from the economic point of view comparing to other existing studies and technologies. The reaction kinetics analysis

demonstrated the dominance of MB over RhB. The most likely reason for this are the different physicochemical properties of the dyes and their state of charge. Methylene blue is a cationic dye, whereas RhB has cationic and zwitterionic forms. RhB degradation is initiated by processes of N-deethylation, chromophore cleavage and ring opening, which result in the generation of oxidation products with smaller molecule sizes. Methylene blue decolorization most likely occurs as a result of the bonding of MB ions with  $S_2O_8^{2-}$  by electrostatic attraction and the subsequent transfer of electrons from MB to the PS. The designed technology is an interesting alternative for dye decolorization compared to other methods presented in literature. Particular advantages of the process include its high dye degradation, low energy consumption and lack of sludge generation.

## 6. Funding sources

The presented study was performed in the framework of the research work in the Central Mining Institute in Poland, financially supported by the Polish Ministry of Science and Higher Education [No. 11131032-340].

## References

- [1] S. Khamparia, D. Jaspal, Technologies for Treatment of Colored Wastewater from Different Industries, C. Hussain, Ed., Handbook of Environmental Materials Management, Springer, Cham, 2018, pp. 1–14. Available at: [https://doi.org/10.1007/978-3-319-58538-3\\_8-1](https://doi.org/10.1007/978-3-319-58538-3_8-1)
- [2] A. Lisiak, M. Miklas, Problem of harmfulness of azo-dyes, *Przełąd Włókienniczy - Włókno, Odzież, Skóra*, nr 3 (2007) 38–40.
- [3] S. Hoenke, I. Serbian, H.-P. Deigner, R. Csuk, Mitocanic di- and triterpenoid Rhodamine B conjugates, *Molecules*, 25 (2020) 5443, doi: 10.3390/molecules25225443.
- [4] W. Chen, J. Mo, X. Du, Z. Zhang, W. Zhang, Biomimetic dynamic membrane for aquatic dye removal, *Water Res.*, 151 (2019) 243–251.
- [5] A.H. Jawad, A.S. Abdulhameed, M.S. Mastuli, Acid-factonized biomass material for methylene blue dye removal: a comprehensive adsorption and mechanism study, *J. Taibah Univ. Sci.*, 14 (2020) 305–313.
- [6] J.A. Malvestiti, E. Fagnani, D. Simão, R.F. Dantas, Optimization of UV/H<sub>2</sub>O<sub>2</sub> and ozone wastewater treatment by the experimental design methodology, *Environ. Technol.*, 40 (2019) 1910–1922.
- [7] W. Zhang, W. Lv, X. Li, J. Yao, Electrochemical oxidative degradation of indigo wastewater based on chlorine-containing system, *Pigm. Resin Technol.*, 49 (2019) 46–54.
- [8] R. Shoukat, S.J. Khan, Y. Jamal, Hybrid anaerobic-aerobic biological treatment for real textile wastewater, *J. Water Process Eng.*, 29 (2019) 100804, doi: 10.1016/j.jwpe.2019.100804.
- [9] U. Roy, S. Manna, S. Sengupta, P. Das, S. Datta, A. Mukhopadhyay, A. Bhowal, Dye Removal Using Microbial Biosorbents, G. Crini, E. Lichtfouse, Eds., *Green Adsorbents for Pollutant Removal: Innovative Materials*, Springer International Publishing, Cham, 2018, pp. 253–280. Available at: [https://doi.org/10.1007/978-3-319-92162-4\\_8](https://doi.org/10.1007/978-3-319-92162-4_8)
- [10] R. Jain, M. Mathur, S. Sikarwar, A. Mittal, Removal of the hazardous dye rhodamine B through photocatalytic and adsorption treatments, *J. Environ. Manage.*, 85 (2007) 956–964.
- [11] D. Kiejza, U. Kotowska, W. Polińska, J. Karpińska, Peroxides - new oxidants in advanced oxidation processes: the use of peracetic acid, peroxymonosulfate, and persulfate salts in the removal of organic micropollutants of emerging concern - a review, *Sci. Total Environ.*, 790 (2021) 148195, doi: 10.1016/j.scitotenv.2021.148195.
- [12] X. Li, B. Jie, H. Lin, Z. Deng, J. Qian, Y. Yang, X. Zhang, Application of sulfate radicals-based advanced oxidation technology in degradation of trace organic contaminants (TrOCs): recent advances and prospects, *J. Environ. Manage.*, 308 (2022) 114664, doi: 10.1016/j.jenvman.2022.114664.
- [13] J. Lee, U. von Gunten, J.-H. Kim, Persulfate-based advanced oxidation: critical assessment of opportunities and roadblocks, *Environ. Sci. Technol.*, 54 (2020) 3064–3081.
- [14] H. Esmaili, A. Kotobi, S. Sheibani, F. Rashchi, Photocatalytic degradation of methylene blue by nanostructured Fe/FeS powder under visible light, *Int. J. Miner. Metall. Mater.*, 25 (2018) 244–252.
- [15] P. Zawadzki, Decolorisation of methylene blue with sodium persulfate activated with visible light in the presence of glucose and sucrose, *Water, Air, Soil Pollut.*, 230 (2019) 313–313.
- [16] M.A. Hassaan, A. El Nemr, F.F. Madkour, A.M. Idris, T.O. Said, T. Sahlabji, M.M. Alghamdi, A.A. El-Zahhar, Advanced oxidation of acid yellow 11 dye; detoxification and degradation mechanism, *Toxin Rev.*, 40 (2021) 1472–1480.
- [17] P.S. Chauhan, K. Kumar, K. Singh, S. Bhattacharya, Fast decolorization of rhodamine-B dye using novel V<sub>2</sub>O<sub>5</sub>-rGO photocatalyst under solar irradiation, *Synth. Met.*, 283 (2022) 116981, doi: 10.1016/j.synthmet.2021.116981.
- [18] M. Yilmaz, N. Mengelizadeh, M. khodadadi Saloot, S. Shahbaksh, D. Balarak, Facile synthesis of Fe<sub>3</sub>O<sub>4</sub>/ZnO/GO photocatalysts for decolorization of acid blue 113 under solar, visible and UV lights, *Mater. Sci. Semicond. Process.*, 144 (2022) 106593, doi: 10.1016/j.mssp.2022.106593.
- [19] M. Chandra, M. Nookaraju, V.K. Sharma, R. Somasekhar, Influence of Vanadium incorporated mesoporous silica on the decolorization of orange G under visible light irradiation, *Inorg. Nano-Metal Chem.*, 52 (2022) 387–396.
- [20] G. Yanagi, M. Furukawa, I. Tateishi, H. Katsumata, S. Kaneco, Electrochemical decolorization of methylene blue in solution with metal doped Ti/α,β-PbO<sub>2</sub> mesh electrode, *Sep. Sci. Technol.*, 57 (2022) 325–337.
- [21] A.S. Al-Shehri, Z. Zaheer, A.M. Alsudairi, S.A. Kosa, Photo-oxidative decolorization of Brilliant Blue with AgNPs as an activator in the presence of K<sub>2</sub>S<sub>2</sub>O<sub>8</sub> and NaBH<sub>4</sub>, *ACS Omega*, 6 (2021) 27510–27526.
- [22] C. Alvarado-Camacho, C.O. Castillo-Araiza, R.S. Ruiz-Martínez, Degradation of Rhodamine B in water alone or as part of a mixture by advanced oxidation processes, *Chem. Eng. Commun.*, 209 (2022) 69–82.
- [23] J. Xie, Y. He, H. Wang, M. Duan, J. Tang, Y. Wang, M. Chamas, H. Wang, Photocatalytic degradation of binary dyes mixture over SrTiO<sub>3</sub> synthesized using sodium carboxymethylcellulose additive, *Russ. J. Phys. Chem.*, 92 (2018) 809–815.
- [24] F. Mahmoudian, F. Nabizadeh Chianeh, S.M. Sajjadi, Simultaneous electrochemical decolorization of Acid Red 33, Reactive Orange 7, Acid Yellow 3 and Malachite Green dyes by electrophoretically prepared Ti/nanoZnO-MWCNTs anode: experimental design, *J. Electroanal. Chem.*, 884 (2021) 115066, doi: 10.1016/j.jelechem.2021.115066.
- [25] C. Wang, Z. Yuan, A. Wang, J. Qu, Z. Fang, Y. Wen, Ultraviolet light enhanced sodium persulfate oxidation of cellulose to facilitate the preparation of cellulose nanofibers, *Cellulose*, 27 (2020) 2041–2051.
- [26] M.Y. Rizal, R. Saleh, A. Taufik, S. Yin, Photocatalytic decomposition of methylene blue by persulfate-assisted Ag/Mn<sub>2</sub>O<sub>4</sub> and Ag/Mn<sub>2</sub>O<sub>4</sub>/graphene composites and the inhibition effect of inorganic ions, *Environ. Nanotechnol. Monit. Manage.*, 15 (2021) 100408, doi: 10.1016/j.enmm.2020.100408.
- [27] D. Maharana, J. Niu, D. Gao, Z. Xu, J. Shi, Electrochemical degradation of Rhodamine B over Ti/SnO<sub>2</sub>-Sb electrode, *Water Environ. Res.*, 87 (2015) 304–311.
- [28] S.G. Pouloupoulos, A. Yerkinova, G. Ulykbanova, V.J. Inglezakis, Photocatalytic treatment of organic pollutants in a synthetic wastewater using UV light and combinations of TiO<sub>2</sub>, H<sub>2</sub>O<sub>2</sub> and Fe(III), *PLoS One*, 14 (2019) e0216745, doi: 10.1371/journal.pone.0216745.
- [29] P. Zawadzki, Evaluation of TiO<sub>2</sub>/UV; O<sub>3</sub>/UV, and PDS/Vis for improving chlorfenvinphos removal from real municipal

- treated wastewater effluent, *Int. J. Environ. Sci. Technol.*, (2022), doi: 10.1007/s13762-022-04370-x.
- [30] J.K. Laha, M.K. Hunjan,  $K_2S_2O_8$  activation by glucose at room temperature for the synthesis and functionalization of heterocycles in water, *Chem. Commun. (Camb.)*, 57 (2021) 8437–8440.
- [31] L. Chu, R. Zhuan, D. Chen, J. Wang, Y. Shen, Degradation of macrolide antibiotic erythromycin and reduction of antimicrobial activity using persulfate activated by gamma radiation in different water matrices, *Chem. Eng. J.*, 361 (2019) 156–166.
- [32] R.J. Watts, M. Ahmad, A.K. Hohner, A.L. Teel, Persulfate activation by glucose for in situ chemical oxidation, *Water Res.*, 133 (2018) 247–254.
- [33] G.V. Buxton, C.L. Greenstock, W.P. Helman, A.B. Ross, Critical review of rate constants for reactions of hydrated electrons, hydrogen atoms and hydroxyl radicals ( $^{\bullet}OH/^{\bullet}O$ ) in aqueous solution, *J. Phys. Chem. Ref. Data*, 17 (1988) 513–886.
- [34] M. Mahanthappa, N. Kottam, S. Yellappa, Enhanced photocatalytic degradation of methylene blue dye using CuScdS nanocomposite under visible light irradiation, *Appl. Surf. Sci.*, 475 (2019) 828–838.
- [35] J. Saien, F. Jafari, Chapter 1 – Methods of Persulfate Activation for the Degradation of Pollutants: Fundamentals and Influencing Parameters, M. Zhu, Z. Bian, C. Zhao, Eds., *Persulfate-based Oxidation Processes in Environmental Remediation*, 2022, 1–59. Available at: <https://doi.org/10.1039/9781839166334-00001>
- [36] M. Bagherzadeh, R. Kaveh, S. Ozkar, S. Akbayrak, Preparation and characterization of a new CdS–NiFe<sub>2</sub>O<sub>4</sub>/reduced graphene oxide photocatalyst and its use for degradation of methylene blue under visible light irradiation, *Res. Chem. Intermed.*, 44 (2018) 5953–5979.
- [37] F. Han, X. Ye, Q. Chen, H. Long, Y. Rao, The oxidative degradation of diclofenac using the activation of peroxymonosulfate by BiFeO<sub>3</sub> microspheres—kinetics, role of visible light and decay pathways, *Sep. Purif. Technol.*, 232 (2020) 115967, doi: 10.1016/j.seppur.2019.115967.
- [38] X. Chen, Z. Xue, Y. Yao, W. Wang, F. Zhu, C. Hong, Oxidation degradation of Rhodamine B in aqueous by treatment system, *Int. J. Photoenergy*, 2012 (2012) e754691, doi: 10.1155/2012/754691.
- [39] L. Urán-Duque, J.C. Saldarriaga-Molina, A. Rubio-Clemente, Advanced oxidation processes based on sulfate radicals for wastewater treatment: research trends, *Water*, 13 (2021) 2445, doi: 10.3390/w13172445.
- [40] A.N. Oliveros, J.A.I. Pimentel, M.D.G. de Luna, S. Garcia-Segura, R.R.M. Abarca, R.-A. Doong, Visible-light photocatalytic diclofenac removal by tunable vanadium pentoxide/boron-doped graphitic carbon nitride composite, *Chem. Eng. J.*, 403 (2021) 126213, doi: 10.1016/j.cej.2020.126213.
- [41] B. Yang, Q. Luo, Q. Li, Y. Meng, L. Lingli, Y. Liu, Selective oxidation and direct decolorization of cationic dyes by persulfate without activation, *Water Sci. Technol.*, 83 (2021) 2744–2752.
- [42] N. Tripathi, Cationic and anionic dye adsorption by agricultural solid wastes: a comprehensive review, *Desalination*, 5 (2013) 91–108.
- [43] W. Li, Z. Jian, Z. Ran, L. Cong, L. Ye, Z. ChengLu, Adsorption of basic dyes on activated carbon prepared from *Polygonum orientale* Linn: equilibrium, kinetic and thermodynamic studies, *Desalination*, 254 (2010) 68–74.
- [44] W. Gao, S. Zhao, H. Wu, W. Deligeer, S. Asuha, Direct acid activation of kaolinite and its effects on the adsorption of methylene blue, *Appl. Clay Sci.*, 126 (2016) 98–106.
- [45] M. Vinuth, H.S.B. Naik, B.M. Vinoda, H. Gururaj, N. Thomas, G. Arunkumar, Enhanced removal of methylene blue dye in aqueous solution using eco-friendly Fe(III)–montmorillonite, *Mater. Today Proc.*, 4 (2017) 424–433.
- [46] S. Sharma, N. Khare, Hierarchical Bi<sub>2</sub>S<sub>3</sub> nanoflowers: a novel photocatalyst for enhanced photocatalytic degradation of binary mixture of Rhodamine B and Methylene blue dyes and degradation of mixture of p-nitrophenol and p-chlorophenol, *Adv. Powder Technol.*, 29 (2018) 3336–3347.
- [47] S. Rani, M. Aggarwal, M. Kumar, S. Sharma, D. Kumar, Removal of methylene blue and rhodamine B from water by zirconium oxide/graphene, *Water Sci.*, 30 (2016), doi: 10.1016/j.wsj.2016.04.001.
- [48] D. Blažeka, J. Car, N. Klobučar, A. Jurov, J. Zavašnik, A. Jagodar, E. Kovačević, N. Krstulović, Photodegradation of Methylene Blue and Rhodamine B using laser-synthesized ZnO nanoparticles, *Materials*, 13 (2020) 4357, doi: 10.3390/ma13194357.
- [49] Z.-H. Diao, J.-J. Liu, Y.-X. Hu, L.-J. Kong, D. Jiang, X.-R. Xu, Comparative study of Rhodamine B degradation by the systems pyrite/H<sub>2</sub>O<sub>2</sub> and pyrite/persulfate: reactivity, stability, products and mechanism, *Sep. Purif. Technol.*, 184 (2017) 374–383.
- [50] C. Lops, A. Ancona, K. Di Cesare, B. Dumontel, N. Garino, G. Canavese, S. Hernández, V. Cauda, Sonophotocatalytic degradation mechanisms of Rhodamine B dye via radicals generation by micro- and nano-particles of ZnO, *Appl. Catal., B*, 243 (2019) 629–640.
- [51] P. Zawadzki, Comparative studies of Rhodamine B decolorization in the combined process Na<sub>2</sub>S<sub>2</sub>O<sub>8</sub>/visible light/ultrasound, *Desal. Water Treat.*, 213 (2021) 269–278.
- [52] M. Mahdavianpour, S. Ildari, M. Ebrahimi, M. Moslemzadeh, Decolorization and mineralization of methylene blue in aqueous solutions by persulfate/Fe<sup>2+</sup> process, *J. Water Chem. Technol.*, 42 (2020) 244–251.
- [53] P. Attri, S. Garg, J.K. Ratan, A.S. Giri, Comparative study using advanced oxidation processes for the degradation of model dyes mixture: reaction kinetics and biodegradability assay, *Mater. Today Proc.*, 57 (2022) 1533–1538.
- [54] H. Heidarpour, M. Padervand, M. Soltanieh, M. Vossoughi, Enhanced decolorization of rhodamine B solution through simultaneous photocatalysis and persulfate activation over Fe/C<sub>3</sub>N<sub>4</sub> photocatalyst, *Chem. Eng. Res. Des.*, 153 (2020) 709–720.
- [55] Y. Pang, K. Luo, L. Tang, X. Li, Y. Song, C. Li, L. Wang, Preparation and application of magnetic nitrogen-doped rGO for persulfate activation, *Environ. Sci. Pollut. Res.*, 25 (2018) 30575–30584.
- [56] R. Jinisha, R. Gandhimathi, S.T. Ramesh, P.V. Nidheesh, S. Velmathi, Removal of rhodamine B dye from aqueous solution by electro-Fenton process using iron-doped mesoporous silica as a heterogeneous catalyst, *Chemosphere*, 200 (2018) 446–454.
- [57] T.S. Natarajan, M. Thomas, K. Natarajan, H.C. Bajaj, R.J. Tayade, Study on UV-LED/TiO<sub>2</sub> process for degradation of Rhodamine B dye, *J. Chem. Eng.*, 169 (2011) 126–134.
- [58] K. Rakesh, S.C. Mohan, S. Karuppachamy, K. Jothivenkatachalam, Photo-assisted advanced oxidation processes for Rhodamine B degradation using ZnO–Ag nanocomposite materials, *J. Environ. Chem. Eng.*, 6 (2018) 3610–3620.
- [59] M.-F. Hou, L. Liao, W.-D. Zhang, X.-Y. Tang, H.-F. Wan, G.-C. Yin, Degradation of rhodamine B by Fe(0)-based Fenton process with H<sub>2</sub>O<sub>2</sub>, *Chemosphere*, 83 (2011) 1279–1283.
- [60] A. Samide, B. Tutunaru, C. Tigae, R. Efrema, A. Moanță, M. Drăgoi, Removal of methylene blue and methyl blue from wastewater by electrochemical degradation, *Environ. Prot. Eng.*, 40 (2014), doi: 10.37190/epe140408.